

**Figure 1.** Molecular structure and atom numbering scheme of *i*-Pr[Cp-1-Flu]HfCl<sub>2</sub>. The atoms are represented by their 50% probability ellipsoids. Important interatomic distances (Å) and bond angles (deg) are as follows: Hf-Cl(1), 2.391 (6); Hf-Cl(2), 2.394 (6); Hf-C(1), 2.40 (2); Hf-C(2), 2.49 (2); Hf-C(3), 2.64 (2); Hf-C(4), 2.64 (2); Hf-C(5), 2.57 (2); Hf-CEN(Flu), 2.24; Hf-CEN(Cp), 2.16; CEN(Flu)-Hf-CEN(Cp), 119.4; C(1)-C(14)-C(17), 101.1. (CEN denotes centroid of a C-5 ring.)

**Table I.** Conditions and Results for Syndiospecific Polymerizations<sup>a</sup>

transition metal, (μmol)	pol. temp, °C	time, min	yield, g	10 <sup>-3</sup> · $\bar{M}_w$	$\bar{M}_w/\bar{M}_n$	rrrr
Zr (1.3)	25	60	26	133	1.9	0.86
Zr (1.3)	50	25	162	69	1.8	0.81
Zr (1.2)	60	60	185	52	1.8	
Zr (1.2) <sup>b</sup>	70	60	158	55	2.4	0.76
Hf (19.2)	50	30	27	777	2.3	0.74
Hf (5.8)	70	60	96	474	2.6	

<sup>a</sup> Propylene (1.2 L); 10 mL of 10.7 wt% methylaluminoxane (MAO) obtained from Shering Industrie-Chemikalien with MW = 1300. <sup>b</sup> MAO (5 mL).

particles with 0.5 g/mL bulk density at 70 °C polymerization temperature. Additional polymerization results are summarized in Table I.

**Polymer C-13 NMR Analyses.** The Zr produced polymers have a ...rrrrrrmmrrrrrrrrrrrrrrrrrr... microstructure with the isotactic triads being the predominant stereochemical defect. The ...rrrrrrmmrrrr... stereosequences indicate site stereochemical control with chain migratory insertions resulting in site isomerizations and occasional reversals in diastereoface selectivity (Scheme I).<sup>6</sup> Catalyst isomerizations independent of monomer addition would result in the meso dyads.

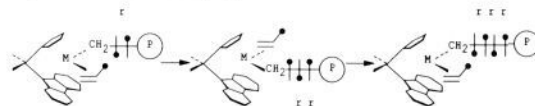
Two percent of the polymer obtained with Hf consists of isotactic blocks. The ...rrrrrrrrmmrrrrrrrrrr... stereoblock microstructure or the isotactic/syndiotactic mixtures are attributed to syndiospecific contact ion pairs and associated neutral, isospecific complexes.

**Concluding Remarks.** The polymerization rates and the polymer molecular weights obtained with the syndiospecific Zr complexes are higher than those obtained with isospecific analogues.<sup>2</sup> The syndiospecific complexes are stereospecific over a wide range of

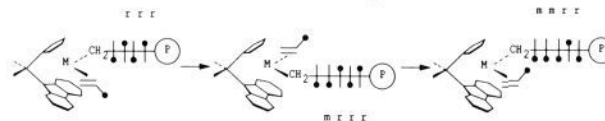
(6) C-13 NMR analysis of a sample with  $\bar{M}_n = 4800$  (GPC) and produced with 100 mg of *i*-PrCp-1-FluZrCl<sub>2</sub> and 5 mL of MAO at 80 °C in pentane at 20 psi propylene showed isopropyl (1.03%), vinylidene (0.51%), and *n*-propyl (0.53%) chain end groups. The absence of vinyl chain ends and the vinylidene chain end groups in a stereoregular environment consistent with the pentad analysis shows that the polymerizations proceed by a 1,2-insertion mechanism as indicated in Scheme I.

### Scheme I

#### Syndiotactic Propagation



#### Reversed Diastereoface Selectivity



polymerization temperatures (Table I), and the "as-polymerized" samples contain little or no atactic polymer under very pure polymerization conditions.

The morphology of the polymer particles indicates the catalysts are propylene insoluble, heterogeneous systems. The narrow polydispersities are typical of chemically homogeneous, active species.

**Supplementary Material Available:** The ligand and metallocene synthetic procedures, polymerization procedure and listings of crystal data, atomic coordinates for hydrogen atoms, bond distances and angles, geometry for the hafnium atoms, best planes, and drawings of the unit cell (48 pages); listing of observed and calculated structure factors (21 pages). Ordering information is given on any current masthead page.

### Correlation of Carbon-13 and Nitrogen-15 Chemical Shifts in Selectively and Uniformly Labeled Proteins by Heteronuclear Two-Dimensional NMR Spectroscopy

William M. Westler,\* Brian J. Stockman, and John L. Markley\*

Department of Biochemistry, College of Agricultural and Life Sciences, University of Wisconsin-Madison  
420 Henry Mall, Madison, Wisconsin 53706

Yoshiko Hosoya, Yoko Miyake, and Masatsune Kainosho

Department of Chemistry, Faculty of Science  
Tokyo Metropolitan University  
Fukazawa, Setagaya-ku, Tokyo, 158 Japan

Received May 11, 1988

Two-dimensional (2D) carbon-13 nitrogen-15 heteronuclear single-bond correlation [<sup>13</sup>C{<sup>15</sup>N}HSBC] spectroscopy<sup>1</sup> has been developed and applied to two double-labeled proteins. The approach has been used with *Streptomyces subtilisin inhibitor* (SSI), a homodimeric protein of reduced molecular mass ( $M_r$ ) 23 000/dimer, labeled uniformly with 60% nitrogen-15 and labeled specifically to 60% carbon-13 at the carbonyl carbons of the three methionine residues,<sup>2</sup> and with *Anabaena* 7120 flavodoxin, a

(1) Successful implementation of <sup>13</sup>C{<sup>15</sup>N}HSBC has been reported recently for <sup>15</sup>N-enriched peptides [Bornemann, V.; Chesnick, A. S.; Helms, G.; Moore, R. E.; Niemczura, W. P. 29th Experimental NMR Conference, Rochester, NY, April 17-21, 1988 (abstract 127)] and proteins [Stockman, B. J.; Westler, W. M.; Mooberry, E. S.; Markley, J. L. 29th Experimental NMR Conference, Rochester, NY, April 17-21, 1988 (abstract 122)]. Westler, W. M.; Kainosho, M.; Nagao, H.; Tomonaga, N.; Markley, J. L. 29th Experimental NMR Conference, Rochester, NY, April 17-21, 1988 (abstract 137). Oh, B. H.; Westler, W. M.; Darba, P.; Markley, J. L. 29th Experimental NMR Conference, Rochester, NY, April 17-21, 1988 (abstract 138)].

(2) [60% <sup>13</sup>C<sup>0</sup> methionine, 60% u-<sup>15</sup>N]SSI was prepared essentially as reported previously<sup>3,4</sup> except that a hydrolyzate of [60% u-<sup>15</sup>N]yeast cells was used instead of an amino acid mixture. The concentration of this hydrolyzate in the culture fluid was 2% in terms of the amino acid mixture. Since the ratio of added DL-[99% atom <sup>1-13</sup>C]Met to [<sup>15</sup>N]Met was approximately two, the expected level of <sup>13</sup>C enrichment is about 60%. (D-Met behaves essentially as L-Met, since racemization is very efficient for this amino acid.) The yield of labeled SSI from a 100-mL culture broth was 16 mg after the usual purification procedures.<sup>3,4</sup>

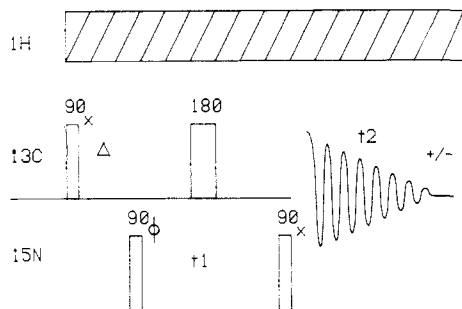


**Figure 1.**  $^{13}\text{C}\{^{15}\text{N}\}$ HSBC pulse sequence. The delay  $\Delta$ , inserted for buildup of antiphase magnetization, was set to  $1/(2 \cdot J_{^{13}\text{C}-^{15}\text{N}})$  with  $J_{^{13}\text{C}-^{15}\text{N}}$  assumed to be 19 Hz. Subsequent studies have shown that better results are obtained in most cases by optimizing the delay for a  $J_{^{13}\text{C}-^{15}\text{N}}$  of 14 Hz. The phase,  $\phi$ , of the first  $^{15}\text{N}$  pulse was inverted every other accumulation, and the results were stored in alternate computer memory locations. The two blocks were subtracted after completion of the experiment. All  $^{13}\text{C}$  pulses were inverted after every two acquisitions, and the results were subtracted from computer memory.

**Table I.**  $^{13}\text{C}$  and  $^{15}\text{N}$  Chemical Shifts and  $^{13}\text{C}$ - $^{15}\text{N}$  One-Bond Coupling Constants in [60%  $^{13}\text{C}^0$  methionine, 60%  $u\text{-}^{15}\text{N}$ ]SSI

dipeptide X-Y	chemical shift (ppm)		coupling constant $J_{^{13}\text{C}-^{15}\text{N}}$ (Hz)	
	$^{13}\text{C}^0$ of residue X	$^{15}\text{N}^a$ of residue Y	from 2D spectrum <sup>a</sup>	from 1D spectra <sup>b</sup>
Met <sup>70</sup> -Cys <sup>71</sup>	174.3	124.3	13.9	15.0
Met <sup>73</sup> -Val <sup>74</sup>	174.2	122.5	15.2	15.2
Met <sup>103</sup> -Asn <sup>104</sup>	175.9	117.5	14.5	14.2

<sup>a</sup> Coupling constants were obtained from rows of the  $^{13}\text{C}\{^{15}\text{N}\}$ HSBC spectrum (Figure 2) which were inverse Fourier transformed, zero filled to eight times the original size, and Fourier transformed again. The error in measurement is estimated to be about 0.1 Hz. <sup>b</sup> Coupling constants were measured from 1D  $^{13}\text{C}$  NMR spectra obtained at 75.4 MHz under solution conditions similar to those used for the 2D experiment. Three separate labeled protein analogues were used to obtain the coupling constants ( $J_{^{13}\text{C}-^{15}\text{N}}$ ): [MC]SSI for Met<sup>70</sup>-Cys<sup>71</sup>, [MV]SSI for Met<sup>73</sup>-Val<sup>74</sup>, and [M,  $u\text{-}^{15}\text{N}$ ]SSI for Met<sup>103</sup>-Asn<sup>104</sup>.<sup>10</sup> The notation [XY]SSI denotes SSI labeled with [ $^{13}\text{C}^0$ ]X and [ $^{15}\text{N}^a$ ]Y, where X and Y stand for the one-letter amino acid abbreviations.

single-chain protein of  $M_r$  21 000, labeled uniformly with 26% carbon-13 and 95% nitrogen-15.<sup>5</sup> The pulse sequence used in the  $^{13}\text{C}\{^{15}\text{N}\}$ HSBC experiment is shown in Figure 1. It is a modification of a pulse sequence originally designed for  $^1\text{H}$  detected heteronuclear chemical shift correlation.<sup>7</sup>

Figure 2 shows the  $^{13}\text{C}\{^{15}\text{N}\}$ HSBC spectrum of [60%  $^{13}\text{C}^0$  methionine, 60%  $u\text{-}^{15}\text{N}$ ]SSI. Peaks appearing in this spectrum result from scalar one-bond coupling between the specifically  $^{13}\text{C}$  labeled methionine carbonyls and the amide  $^{15}\text{N}$  of the following amino acid residue. Sequence-specific assignments of the methionine  $^{13}\text{C}^0$  resonances in SSI were obtained previously by a dual labeling strategy and one-dimensional (1D) NMR analysis.<sup>3,4,8</sup> These assignments allow the immediate assignment of the  $^{15}\text{N}$  signals from residues X in the three Met-X dipeptides in the protein sequence:<sup>9</sup> Met<sup>70</sup>-Cys<sup>71</sup>, Met<sup>73</sup>-Val<sup>74</sup>, and Met<sup>103</sup>-Asn<sup>104</sup> (Table I). The coupling constants in Table I were obtained from slices of the 2D NMR spectrum; they are consistent with those based on 1D NMR results,<sup>10</sup> except for Met<sup>70</sup>-Cys<sup>71</sup> where the

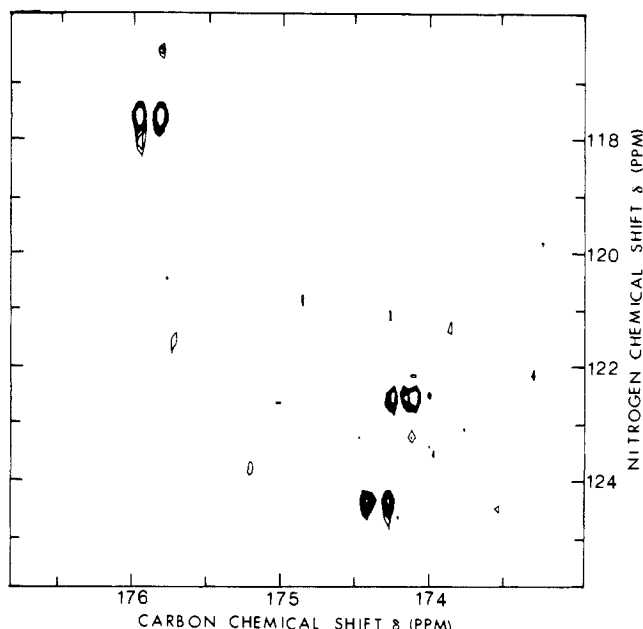


**Figure 2.** The  $^{13}\text{C}\{^{15}\text{N}\}$ HSBC spectrum of [60%  $^{13}\text{C}^0$  methionine, 60%  $u\text{-}^{15}\text{N}$ ]SSI. The sample was 16 mg of protein dissolved in 1.2 mL of 50 mM phosphate buffer at pH 7.3 in 90%  $\text{H}_2\text{O}/10\% \text{ }^2\text{H}_2\text{O}$ . The sample was placed in a 1.2-mL microcell (Wilma Glass) that was inserted into a standard 10 mm OD NMR tube. The temperature of the sample was held at 61  $^\circ\text{C}$ . The  $^{15}\text{N}$  frequency (40.55 MHz) was set at the high field end of the  $^{15}\text{N}$  spectrum, and the  $^{13}\text{C}$  frequency (100.6 MHz) was located at the center of the  $^{13}\text{C}$  spectrum. Real Fourier transforms were performed in both  $\omega_2$  and  $\omega_1$  dimensions. The Bruker AM-400 BSV7 transmitter was used to supply the  $^{13}\text{C}$  frequency, and a BSV3 X-nucleus decoupler was used for the  $^{15}\text{N}$  frequencies. Protons were decoupled by composite pulse decoupling with standard Bruker hardware. The 10 mm NMR probe with  $^1\text{H}$ ,  $^{13}\text{C}$ , and  $^{15}\text{N}$  channels and a  $^2\text{H}$  lock channel was purchased from Bruker. Carbon-13 chemical shifts were calibrated against external aqueous dioxane at 61  $^\circ\text{C}$  which was assigned a chemical shift of 67.8 ppm from ( $^{13}\text{CH}_3$ )<sub>4</sub>Si. Nitrogen-15 chemical shifts were calibrated against external ammonium sulfate at 61  $^\circ\text{C}$  which was assigned a chemical shift of 21.6 ppm from liquid ammonia.

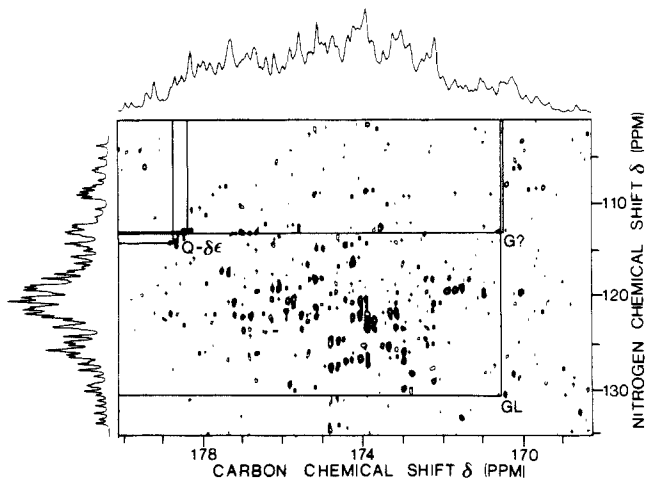


**Figure 3.** The  $^{13}\text{C}\{^{15}\text{N}\}$ HSBC spectrum of [26%  $u\text{-}^{13}\text{C}$ , 95%  $u\text{-}^{15}\text{N}$ ]-flavodoxin from *Anabaena* 7120. The carbonyl carbon region is shown. The sample, containing 2.1 mM protein and 100 mM potassium phosphate dissolved in 90%  $\text{H}_2\text{O}/10\% \text{ }^2\text{H}_2\text{O}$  at pH 7.5, was placed in a cylindrical microcell (total volume 1.2 mL) that was inserted into a standard 10 mm OD NMR tube. Data acquisition and chemical shift references were as described in the legend to Figure 2, except that the temperature of the sample (and external references) was 27  $^\circ\text{C}$ . Cross-peaks representing peptide bond connectivities are indicated for two glycine residues (GL and G?). Two glutamine side-chain connectivities also are identified (Q- $\delta\epsilon$ ).

discrepancy appears to exceed experimental error for reasons unknown at present.

(3) Kainosho, M.; Tsuji, T. *Biochemistry* **1982**, *21*, 6273-6279.

(4) Kainosho, M.; Nagao, H.; Tsuji, T. *Biochemistry* **1987**, *26*, 1068-1075.

(5) Flavodoxin was enriched by growing the cyanobacteria on sole carbon and nitrogen sources of [26%  $^{13}\text{C}$ ]CO<sub>2</sub> and [95%  $^{15}\text{N}$ ]KNO<sub>3</sub>, respectively. Culture and purification procedures were as described previously.<sup>6</sup>

(6) Stockman, B. J.; Westler, W. M.; Mooberry, E. S.; Markley, J. L. *Biochemistry* **1988**, *27*, 136-142.

(7) Bax, A.; Griffey, R. H.; Hawkins, B. L. *J. Magn. Reson.* **1983**, *55*, 301-315.

(8) Kainosho, M.; Nagao, N.; Imamura, Y.; Uchida, K.; Tomonaga, N.; Nakamura, Y.; Tsuji, T. *J. Mol. Struct.* **1985**, *126*, 549-562.

(9) Ikenaka, T.; Odani, S.; Sakai, M.; Nabeshima, Y.; Sato, S.; Murao, S. *J. Biochem. (Tokyo)* **1974**, *76*, 1191-1209.

Figure 3 shows the  $^{13}\text{C}\{^{15}\text{N}\}$ HSBC spectrum of [26% u- $^{13}\text{C}$ , 95% u- $^{15}\text{N}$ ]flavodoxin from *Anabaena* 7120. A number of peaks have been assigned to specific types of  $^{13}\text{C}$ - $^{15}\text{N}$  connectivities, and one  $^{13}\text{C}^0$ - $^{15}\text{N}^\alpha$  cross-peak has been assigned to a specific dipeptide. The cross-peaks labeled Q- $\delta\epsilon$  (178.4 ppm  $^{13}\text{C}$ , 113.1 ppm  $^{15}\text{N}$  and 178.7 ppm  $^{13}\text{C}$ , 114.2 ppm  $^{15}\text{N}$ ) have been assigned to glutamine side-chain amide groups. These are distinguished from backbone amides by two kinds of information: (a) peaks at the corresponding  $^{13}\text{C}$  chemical shifts in the  $^{13}\text{C}\{^{13}\text{C}\}$  double quantum correlated [ $^{13}\text{C}\{^{13}\text{C}\}$ DQC] spectrum<sup>11</sup> are identified as belonging to side-chain carbonyls in either aspartic acid or glutamine residues; (b) the corresponding  $^{15}\text{N}$  peaks in the  $^{15}\text{N}$  INEPT spectrum show modulation behavior consistent with  $^{15}\text{N}$  nuclei bound to two  $^1\text{H}$  nuclei.<sup>6</sup> The  $^{13}\text{C}$  chemical shift of the peak labeled G? (170.4 ppm  $^{13}\text{C}$ , 113.3 ppm  $^{15}\text{N}$ ) is assigned to a glycine spin system on the basis of  $^{13}\text{C}\{^{13}\text{C}\}$ DQC data; hence the  $^{13}\text{C}\{^{15}\text{N}\}$ HSBC cross-peak is assigned to coupling between a glycine  $^{13}\text{C}^0$  and the  $^{15}\text{N}$  amide of the next amino acid residue in the protein. A similar argument was used to assign the peak labeled GL (170.5 ppm  $^{13}\text{C}$ , 131.2 ppm  $^{15}\text{N}$ ) to coupling between the  $^{13}\text{C}^0$  of a glycine and the amide  $^{15}\text{N}$  of the next amino acid residue. The amide  $^{15}\text{N}$  was assigned to a leucine residue by identifying the single  $^1\text{H}\{^{15}\text{N}\}$ -HSBC cross-peak at this  $^{15}\text{N}$  frequency<sup>6</sup> as belonging to a leucine spin system on the basis of  $^1\text{H}\{^1\text{H}\}$  correlation spectroscopy (not shown). Thus the  $^{13}\text{C}\{^{15}\text{N}\}$ HSBC cross-peak corresponds to a glycyl-leucyl dipeptide in the flavodoxin. Since the amino acid sequence for this protein has not been determined, the dipeptide cannot be assigned to a specific position in the sequence.

The present results show the utility of the  $^{13}\text{C}\{^{15}\text{N}\}$ HSBC 2D NMR experiment for making sequence-specific assignments and identifying signals from side-chain amides in isotopically labeled proteins of moderate size ( $M_r$  21 000 to 23 000). The detection of  $^{13}\text{C}^0$ - $^{15}\text{N}^\alpha$  bonds by 2D NMR spectroscopy will support new strategies for sequence-specific assignments that require fewer isotopically labeled protein analogues than the original dual-labeling strategy.<sup>3,4,8</sup> The multiple scalar coupling pathways afforded by a combination of  $^{13}\text{C}\{^{15}\text{N}\}$ HSBC spectroscopy with  $^{13}\text{C}\{^{13}\text{C}\}$ -DQC,<sup>11-13</sup> heteronuclear single-bond and multiple-bond  $^1\text{H}\{^{13}\text{C}\}$  2D spectroscopy,<sup>13</sup> and  $^1\text{H}\{^1\text{H}\}$  2D spectroscopy<sup>14</sup> form a powerful set of tools for the assignment of nearly all spin 1/2 nuclei in macromolecules of moderate size. These strategies for sequence-specific assignments are based on scalar coupling, unlike those for  $^1\text{H}\{^1\text{H}\}$  2D NMR which require detection of interresidue nuclear Overhauser effects. These new methods should prove useful in studies of proteins whose analysis by  $^1\text{H}\{^1\text{H}\}$  2D NMR methods is impractical because of their large size or spectral complexity.

**Acknowledgment.** We thank Dr. E. S. Mooberry for assistance with NMR instrumentation and Dr. M. D. Reily for help with sample preparation. This study was supported by USDA Grant 85-CRCR-1-1589, NIH Grant RR02301, and grants in aid from the Ministry of Education of Japan (60430033, 60880022, 62220026). Spectroscopy was performed at the National Magnetic Resonance Facility at Madison which is funded by National Institutes of Health Grant RR02301 from the Biomedical Research Technology Program, Division of Research Resources and the University of Wisconsin. Additional support for equipment came from the NSF Biological Biomedical Research Technology Program (DMB 8415048), the NIH Shared Instrumentation Program (RR02781), and the U. S. Department of Agriculture. B.J.S. is supported by an NIH Training Grant in Cellular and Molecular Biology (GM07215).

(10) Hosoya, Y.; Miyake, Y.; Tsukahara, S.; Kainosho, M., unpublished data.

(11) Stockman, B. J.; Westler, W. M.; Darba, P.; Markley, J. L. *J. Am. Chem. Soc.* **1988**, *110*, 4095-4096.

(12) Oh, B. H.; Westler, W. M.; Darba, P.; Markley, J. L. *Science (Washington, D.C.)* **1988**, *240*, 908-911.

(13) Westler, W. M.; Kainosho, M.; Nagao, H.; Tomonaga, N.; Markley, J. L. *J. Am. Chem. Soc.* **1988**, *110*, 4093-4095.

(14) Wüthrich, K. *NMR of Proteins and Nucleic Acids*; Wiley-Interscience: New York, 1986.

## Mass Measurements Using Isotopically Labeled Solvents Reveal the Extent of Solvent Transport during Redox in Thin Films on Electrodes

Steven J. Lasky and Daniel A. Buttry\*

Department of Chemistry, University of Wyoming  
Laramie, Wyoming 82071

Received April 28, 1988

Revised Manuscript Received July 5, 1988

Transport of solvent during the redox reactions of thin films on electrodes has been identified as a possible influence on both the thermodynamic and kinetic aspects of their electrochemical responses.<sup>1</sup> A variety of methods has been used in attempts to measure solvent content of these films, including ellipsometry<sup>2,3</sup> and profilometry.<sup>4</sup> However, those techniques which rely on measurement of thickness suffer from inability to deconvolute the contributions to swelling (or deswelling) from ion and solvent transport. Thus, the situation remains one in which speculation abounds, but accurate measurements are unavailable. In this communication, we report on the application of the quartz crystal microbalance (QCM) technique to the determination of solvent transport during redox in thin films of nickel ferrocyanide (the nickel analogue of Prussian Blue<sup>5-12</sup>) by comparing the difference in the total mass change (comprised of contributions from both ion and solvent transport) which results from use of isotopically substituted solvent. To our knowledge, these experiments represent the first accurate, unambiguous measurements of solvent transport in thin films on electrodes. It is especially significant that these measurements are made in the presence of simultaneous ion transport.

The QCM apparatus has been previously described.<sup>13-15</sup> When used in conjunction with electrochemical measurements, it allows for the simultaneous determination of minute (multilayer to submonolayer) mass changes which accompany the electrochemical reaction with a mass sensitivity of 56.6 Hz/microgram/cm<sup>2</sup> in the present experimental configuration. Nickel films were deposited onto the QCM gold electrode either by using a modified Watts bath<sup>16</sup> or by vapor deposition with identical results. The nickel ferrocyanide films were generated by using the method of Bocarsly and co-workers,<sup>7</sup> by maintaining the electrode potential at 1.2 V in a solution of 0.1 M KCl and 0.01 M K<sub>4</sub>Fe(CN)<sub>6</sub> for the time required to obtain the desired film thickness. Conditions were precisely controlled to ensure uniformity of the deposited films, since this is crucial for the quantitative comparison of the QCM frequency change (which gives the mass change) to the electrochemical charge.<sup>17</sup> FTIR microscopy (Mattson Cygnus

(1) Murray, R. W. In *Electroanalytical Chemistry*; Bard, A. J., Ed.; Marcel Dekker: New York, 1984; Vol. 13, p 191.

(2) (a) Carlin, C. M.; Kopley, L. J.; Bard, A. J. *J. Electrochem. Soc.* **1985**, *132*, 353-9. (b) Winston, G. C.; Carlin, C. M. *J. Electrochem. Soc.* **1988**, *135*, 789-90.

(3) Gottesfeld, S.; Redondo, A.; Feldberg, S. W. *J. Electrochem. Soc.* **1987**, *134*, 271.

(4) Lewis, T. J.; White, H. S.; Wrighton, M. S. *J. Am. Chem. Soc.* **1984**, *106*, 6947-52.

(5) Bocarsly, A. B.; Sinha, S. *J. Electroanal. Chem.* **1982**, *137*, 157-62.

(6) Bocarsly, A. B.; Sinha, S. *J. Electroanal. Chem.* **1982**, *140*, 167-72.

(7) Sinha, S.; Humphrey, B. D.; Bocarsly, A. B. *Inorg. Chem.* **1984**, *23*, 203-12.

(8) Humphrey, B. D.; Sinha, S.; Bocarsly, A. B. *J. Phys. Chem.* **1984**, *88*, 736-43.

(9) Sinha, S.; Humphrey, B. D.; Fu, E.; Bocarsly, A. B. *J. Electroanal. Chem.* **1984**, *162*, 351-7.

(10) Amos, L. J.; Schmidt, M. H.; Sinha, S.; Bocarsly, A. B. *Langmuir* **1986**, *2*, 559-61.

(11) Sinha, S.; Amos, L. J.; Schmidt, M. H.; Bocarsly, A. B. *J. Electroanal. Chem.* **1986**, *210*, 323-8.

(12) Humphrey, B. D.; Sinha, S.; Bocarsly, A. B. *J. Phys. Chem.* **1987**, *91*, 586-93.

(13) Melroy, O. R.; Kanazawa, K. K.; Gordon, J. G.; Buttry, D. A. *Langmuir* **1986**, *2*, 697-700.

(14) Orata, D. O.; Buttry, D. A. *J. Am. Chem. Soc.* **1987**, *109*, 3574-81.

(15) Varineau, P. T.; Buttry, D. A. *J. Phys. Chem.* **1987**, *91*, 1292-5.

(16) Hoare, J. P. *J. Electrochem. Soc.* **1986**, *133*, 2491-4.